

# Bifurcation Diagram of the Oscillatory Belousov-Zhabotinskii System of Oxalic Acid in a Continuous Flow Stirred Tank Reactor. Further Possible Evidence of Saddle Node Infinite Period Bifurcation Behavior of the System

V. Gáspár\* and P. Galambosi

Department of Physical Chemistry, Institute of Chemistry, Kossuth Lajos University, Debrecen, H-4010, Hungary (Received: November 4, 1985; In Final Form: January 15, 1986)

This paper presents the bifurcation diagram of one of the simplest Belousov-Zhabotinskii (BZ) type oscillators (the bromate-cerium-oxalic acid system) in a continuous flow stirred tank reactor (CSTR). The results support that the transitions from steady states to periodic orbits, and vice versa, proceed via saddle node infinite period (SNIPER) bifurcations. This finding agrees with the results in batch when the produced bromine was removed by an inert gas stream (Noszticzius et al.). Computations demonstrate that a simple revised Oregonator type and bromine-hydrolysis-controlled model cannot describe the SNIPER bifurcation behavior of the system in a CSTR.

## Introduction

The bromate-cerium-oxalic acid oscillatory system<sup>1,2</sup> is one of the simplest Belousov-Zhabotinskii (BZ) type oscillators, since the organic component cannot be brominated. Consequently, the produced bromine has to be removed for sustaining the oscillation. The removal can be performed in different ways: (a) by bubbling inert gas<sup>1,2</sup> through the system, (b) in a flow-through reactor,<sup>3</sup> and (c) chemically (for example, by adding acetone<sup>4</sup>). Ševčík and Adamčíková<sup>3</sup> have recently demonstrated that at a given composition the oscillation period is largely determined by the removal rate of bromine, independent of the method of removal.

In spite of the intensive studies, the mechanistic details of this simple system are still far from being complete. In light of the experiments of Noszticzius et al.<sup>5</sup> it is now clear that there is no possibility of explaining the oscillation in this system by a direct bromine-controlled mechanism (Explodator<sup>6</sup>). Although Bódiss and Field<sup>7a</sup> succeeded in modeling one of the original experiments of Noszticzius and Bódiss<sup>1</sup> on the basis of a revised Oregonator type<sup>8,9</sup> and bromide-hydrolysis-controlled model,<sup>7b</sup> however, preliminary calculations indicate<sup>10</sup> that such a type of mechanism cannot describe the experimentally determined SNIPER bifurcations in batch when bromine is removed by method a (Noszticzius et al.<sup>11</sup>).

Maseřko<sup>12</sup> described how the four types of theoretically classified<sup>13</sup> bifurcations (leading from simple steady states to periodic orbits, and vice versa) can be distinguished experimentally. One should determine the dependence of time period and amplitude of the periodic orbits on a bifurcation parameter and detect the

absence or presence of hysteresis during the transition processes.

Recent results of Noszticzius et al.<sup>11</sup> have unambiguously shown the occurrence of SNIPER bifurcations in batch reactions. Moreover, the two different theoretically predicted excitable steady states that are connected the range of oscillations were also detected by the perturbation technique. Since oxalic acid is consumed with a moderate rate under batch conditions and thus the system is not a real open one, there is a drift in the amplitude and the time period of oscillations. The parameters consistent with the initial conditions had to be calculated by an extrapolation to  $t = 0$ . Such an extrapolation gives, however, less precise data than that of an ideal open system.

A flow-through system is a better approximation to this ideal case because of the constant influx of the fresh reactants. According to the results of Ševčík and Adamčíková,<sup>3</sup> the occurrence of SNIPER bifurcations can also be predicted under CSTR conditions.

We intended to check this prediction and to compare the experiments with the results of computations according to a revised Oregonator type<sup>8,9</sup> and bromine-hydrolysis-controlled model<sup>7b</sup> of the bromate-cerium-oxalic acid system under CSTR conditions.

## Experimental Section

All chemicals were reagent grade products (KBrO<sub>3</sub> and H<sub>2</sub>-C<sub>2</sub>O<sub>4</sub>·2H<sub>2</sub>O, Reanal; Ce(SO<sub>4</sub>)<sub>2</sub>·4H<sub>2</sub>O, Merck; H<sub>2</sub>SO<sub>4</sub> (96%), Carlo Erba). Potassium bromate was recrystallized from hot sulfuric acid solution (1.0 mol dm<sup>-3</sup>). Under such conditions the bromide ion contamination is quickly removed by the reaction between bromate and bromide ions producing bromine. The resultant crystals were separated by filtration, washed with water, and dried. The concentration of the stock solution was determined by the standard iodometric method.

The experimental setup for CSTR was similar to that reported earlier.<sup>14</sup> Bright-platinum and bromide-selective electrodes were applied for monitoring the redox potential and the concentration of bromide ion. Since there were only two input tubes in the CSTR, the components could not be input into the reactor separately. Two of them had to be premixed in one of the two reservoirs. In most of the experiments the two input solutions were as follows: solution A, potassium bromate in 1.0 M H<sub>2</sub>SO<sub>4</sub>; solution B, (cerium sulfate + oxalic acid) in 1.0 M H<sub>2</sub>SO<sub>4</sub>. Since the analytical concentration of oxalic acid was always much higher than that of the cerium sulfate, it was thus reduced to cerous completely. Freshly prepared mixtures of potassium bromate and oxalic acid were also applied at the beginning. Later on in the

(1) Noszticzius, Z.; Bódiss, J. *J. Am. Chem. Soc.* **1979**, *101*, 3177-3182.

(2) Ševčík, P.; Adamčíková, L. *Collect. Czech. Chem. Commun.* **1983**, *47*, 891-898.

(3) Ševčík, P.; Adamčíková, L. *Collect. Czech. Chem. Commun.* **1985**, *50*, 799-805.

(4) Noszticzius, Z. *Magy. Kem. Foly.* **1979**, *85*, 330-331.

(5) Noszticzius, Z.; Gáspár, V.; Försterling, H. D. *J. Am. Chem. Soc.* **1985**, *107*, 2314-2315.

(6) Noszticzius, Z.; Farkas, H.; Schelly, Z. A. *J. Chem. Phys.* **1984**, *80*, 6062-6070.

(7) (a) Bódiss, J.; Field, R. J. In *Oscillations and Traveling Waves in Chemical Systems*; Field, R. J., Burger, M., Eds.; Wiley-Interscience: New York, 1985; Chapter 2, p 70. (b) Field, R. J. In ref 7a; p 69.

(8) Noyes, R. M. *J. Chem. Phys.* **1984**, *80*, 6071-6078.

(9) Tyson, J. J. *J. Chem. Phys.* **1984**, *80*, 6079-6082.

(10) Gáspár, V.; Noszticzius, Z.; Farkas, H., submitted for publication in *React. Kinet. Catal. Lett.*

(11) Noszticzius, Z.; Stirling, P.; Wittmann, M. *J. Phys. Chem.* **1985**, *89*, 4914-4921.

(12) Maseřko, J. *Chem. Phys.* **1982**, *67*, 17-26.

(13) Andronov, A. A.; Vitt, A. A.; Khaikin, S. E. *Theory of Oscillators*; Pergamon: Oxford, 1966.

(14) Gáspár, V.; Bazsa, G.; Beck, M. T. *J. Phys. Chem.* **1985**, *89*, 5495-5499.

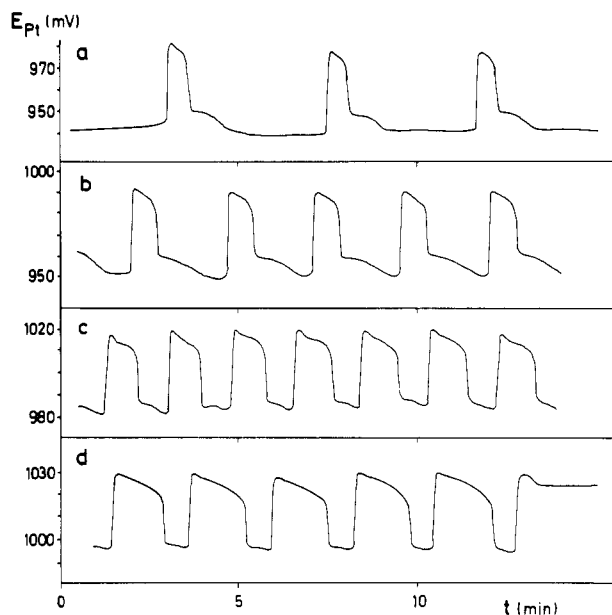
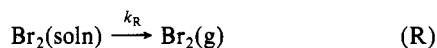


**Figure 1.** Platinum electrode potential oscillations at different input concentrations of bromate ion with  $[\text{H}_2\text{SO}_4]_0 = 1.0 \text{ M}$ ,  $[(\text{COOH})_2]_0 = 1.25 \times 10^{-2} \text{ M}$ ,  $[\text{Ce(III)}]_0 = 6.5 \times 10^{-4} \text{ M}$ , and  $k_0 = 6.8 \times 10^{-3} \text{ s}^{-1}$ . Values of  $[\text{BrO}_3^-]_0$  were (a)  $3.75 \times 10^{-2} \text{ M}$ , (b)  $4.0 \times 10^{-2} \text{ M}$ , (c)  $5.0 \times 10^{-2} \text{ M}$ , and (d)  $5.5 \times 10^{-2} \text{ M}$ .  $[\text{X}]_0$ : Here and hereafter the input concentrations are given in the reactor after mixing but before any reaction takes place.

systematic study this variation was neglected because of the considerable effect of the well-known reaction<sup>15</sup> between these components. The actual input concentrations of components (indicated by the symbol  $[\ ]_0$ ) and the flow rate ( $k_0 = 1/\tau$ , where  $\tau$  is the mean residence time of the component in the reactor) are shown in the figures.

The bifurcation diagram of the system at an appropriate flow rate and fixed concentrations of cerous ion and sulfuric acid was measured as follows: at a given input concentration of oxalic acid (ranging from  $5 \times 10^{-4}$  to  $10^{-1} \text{ M}$ ) the input concentration of bromate ion was increased and decreased gradually. By this method the different regions of the oxalic acid–bromate constraint–constraint space could be divided easily. The changes in potentials of platinum and bromide-selective electrodes were followed for at least  $3-5\tau$  time, until a steady state or an oscillatory state was reached.

Since a gaseous product, bromine, is formed in the reaction, its evaporation and also the effect of the aspirator applied to drain the excess of solution from the CSTR cannot be neglected.<sup>14</sup> They can result in an independent bromine removal. We found that the concentration of a bromine solution decreases by a formally first-order reaction R.



The rate constant  $k_R$  was determined under the experimental conditions by modification of the potentiometric method developed by Noszticzus et al.<sup>11</sup> (We applied a saturated calomel electrode as a reference.)  $k_R$  was found to be  $5 \times 10^{-3} \text{ s}^{-1}$ .

The temperature was held constant ( $T = 298 \pm 0.1 \text{ K}$ ).

## Results and Discussion

The bromate–cerium–oxalic acid BZ system in CSTR shows small-amplitude oscillations in both measured potentials within broad regions of various constraint parameters such as the input concentration of different components and the flow rate  $k_0$ . However, the shapes of the oscillatory curves change as soon as the value of the chosen constraint parameter is modified. Figures 1 and 2 show such types of peculiar changes in the character of

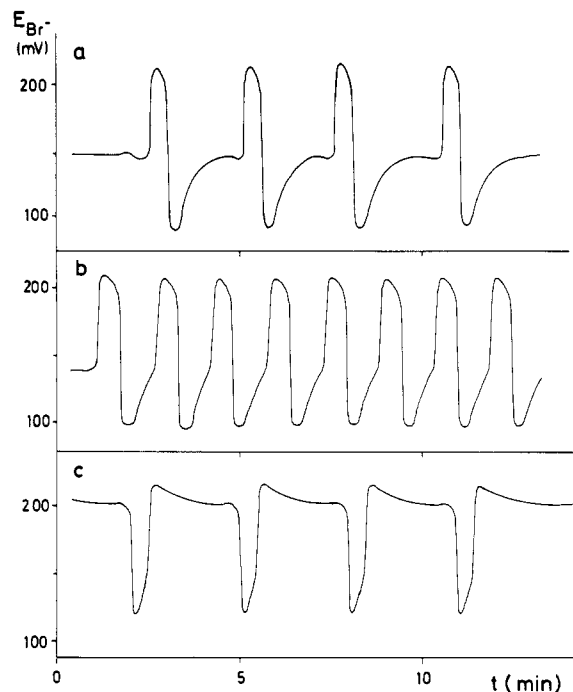


**Figure 2.** Bromide-selective electrode potential oscillations at different input concentrations of bromate ion with  $[(\text{COOH})_2]_0 = 2.5 \times 10^{-2} \text{ M}$ . The other parameters are the same as in Figure 1. Values of  $[\text{BrO}_3^-]_0$  were (a)  $4.25 \times 10^{-2} \text{ M}$ , (b)  $5.0 \times 10^{-2} \text{ M}$ , and (c)  $6.75 \times 10^{-2} \text{ M}$ .

the potential oscillations measured by platinum and bromide-selective electrodes, respectively, when, for instance, only the input concentration of bromate ion is increased. (Similar changes can be detected when the flow rate  $k_0$  is increased gradually.  $k_0$  is a control parameter analogous to the velocity of gas stream in batch experiments.) It is apparent from Figures 1 and 2 that the amplitudes of the limit cycle type oscillations in both potentials are approximately constant (40 and  $\sim 100 \text{ mV}$  in platinum and bromide-selective electrodes, respectively), although there are slow drifts in the lower and upper limits of the potential values. It can also be detected that the time periods of oscillations go through minimum values in both cases depicted in Figures 1 and 2. In accordance with the general theory of bromate-driven oscillators,<sup>8</sup> the changes in the cerium(IV) and bromide concentrations take place nearly in contrast to each other, which means that when the concentration of Ce(IV) is high, the concentration of bromide ion is very low, and vice versa. Since these two components are strongly coupled, it is enough to apply only one type, for instance, the platinum potential–time curves, for characterizing the system. The low- and high-potential stages of these curves will be indicated by “L” and “H”, respectively.

It is clear from Figures 1 and 2 that upon increasing the input concentration of bromate ion, the system spends less and less time near the L state and thus more and more time near the H state during a period of oscillation. This is a consequence of the peculiar “deformation” of the limit cycle in the many-dimensional space.

These results are in complete agreement with the batch experiments<sup>11</sup> and qualitatively indicate the possibility of SNIPER bifurcation under CSTR conditions, too.

For a quantitative study we applied to the system the so-called “crossed-shape phase diagram” method<sup>16</sup> by choosing two main components (bromate ion and oxalic acid) as the constraint parameters.

Figure 3 shows the bifurcation diagram of the system. It is similar to the same type of diagrams of other bromate-driven oscillators (for example ref 12, 14, 17, and 18). There are four

(16) Boissonade, J.; DeKepper, P. *J. Phys. Chem.* **1980**, *84*, 501–506.

(17) Orbán, M.; DeKepper, P.; Epstein, I. R. *J. Am. Chem. Soc.* **1982**, *104*, 2657–2658.

(18) Alamgir, M.; Orbán, M.; Epstein, I. R. *J. Phys. Chem.* **1983**, *87*, 3725–3728.

(15) Ševčík, P.; Adamčíková, L.; Gunárová, D.; Kováčiková, D. *Acta Fac. Rerum Nat. Univ. Comenianae, Chimia* **1983**, *31*, 17–28.

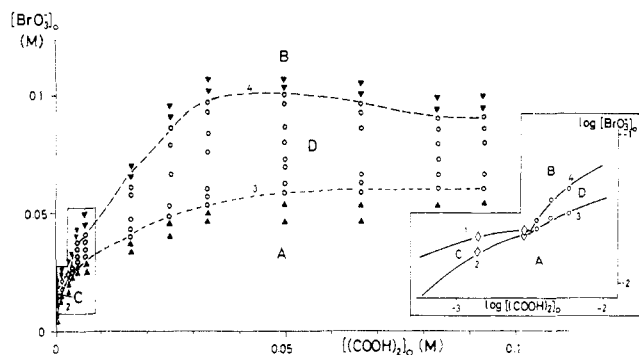


**Figure 3.** Bifurcation diagram for bromate-cerium-oxalic acid system at  $[\text{H}_2\text{SO}_4]_0 = 1.0 \text{ M}$ ,  $[\text{Ce(III)}]_0 = 4.3 \times 10^{-4} \text{ M}$ , and  $k_0 = 4.5 \times 10^{-3} \text{ s}^{-1}$ : ▲, steady state "L"; ▼, steady state "H"; ◊, bistability; ○, oscillation.

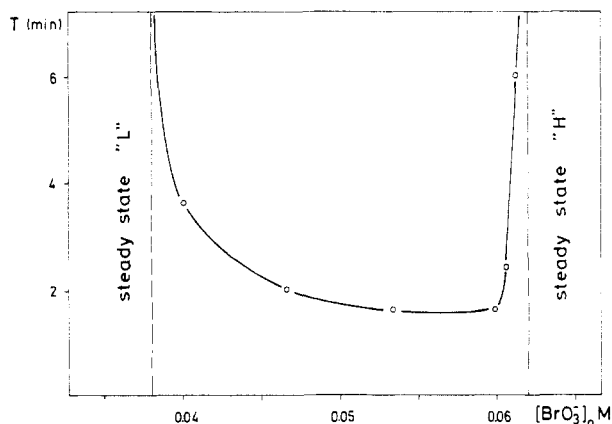


**Figure 4.** Dependence of time period on the input concentration of bromate ion.  $[(\text{COOH})_2]_0 = 1.66 \times 10^{-2} \text{ M}$  and the other parameters are the same as in Figure 3.

parts in the plot. Regions A and B correspond to the monostable steady states L and H, respectively. Curve 1 indicates the transition from L state to H state, while at curve 2 the opposite transition occurs. Between these curves the system exhibits bistability (region C). Curves 3 and 4 correspond to the transitions from monostable steady states to the oscillatory state (region D), and vice versa, *without experimentally detectable hysteresis*. As shown in Figure 3, the resolution of the search was quite fine ( $0.005 \text{ mol dm}^{-3}$  or less difference in bromate inflow concentrations).

According to the theory,<sup>12,13</sup> the absence of hysteresis during these transitions (curves 3 and 4) is connected to either the supercritical Hopf's or the SNIPER bifurcations. Figures 4 and 5 show the changes of time period and amplitude (depicted here only in bromide-selective electrode potential), respectively, in a given segment of the bifurcation diagram. Similar curves were found in the whole oscillatory region. (See also Figure 8.) As it is shown, the time period tends to infinity near the limits of the oscillatory region in bromate ion concentration and the amplitude is almost constant in the same region. (We agree with one of our reviewers that it is not easy to prove experimentally that the time period tends to infinity close to the borders. The finest resolution of the search for the type of the bifurcation would be a nearly continuous change of a bifurcation parameter, like the flow rate. Nevertheless, the tendency of our results and also the good agreement with the results in batch<sup>11</sup> are indicative of a SNIPER bifurcation.)

By these quantitative observations it can be concluded that the prediction in the Introduction was right. The transitions from steady states to periodic orbits, and vice versa, proceed via SNIPER bifurcations in CSTR, too.

The existence of SNIPER bifurcation can be confirmed by investigation of the excitability of steady states with perturbation experiments in the vicinity of the bifurcation points. One type of perturbation which can easily be performed in a CSTR is the stopping of the inflow for small intervals. This method can be

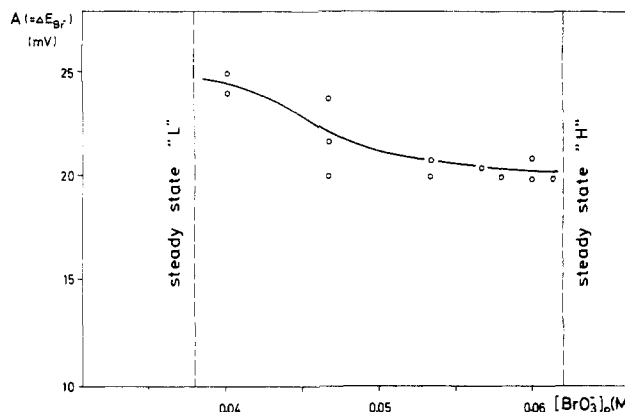


**Figure 5.** The effect of the input concentration of bromate ion on the amplitude of oscillation in the potential of bromide-selective electrode. The parameters are the same as in Figure 4.

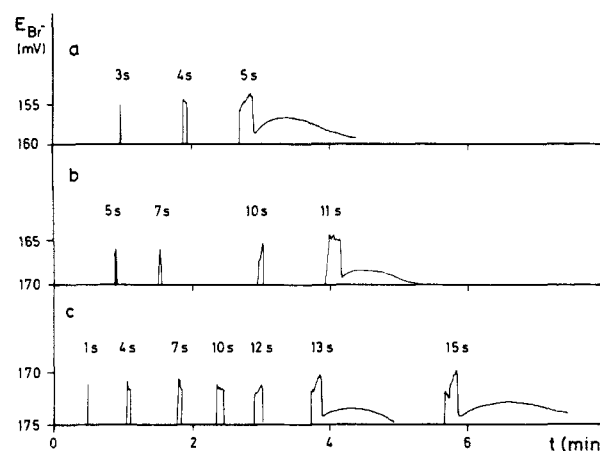


**Figure 6.** Experimental evidence on the excitability of the H steady state of the system. The relaxation curves were measured by means of a bromide-selective electrode following the perturbations produced by stopping of the inflow for different intervals (seconds). Constraints:  $[(\text{COOH})_2]_0 = 5 \times 10^{-3} \text{ M}$  and the others are the same as in Figure 3. Values of  $[\text{BrO}_3^-]_0$  were (a)  $3.33 \times 10^{-2} \text{ M}$ , (b)  $4 \times 10^{-2} \text{ M}$ , and (c)  $5.33 \times 10^{-2} \text{ M}$ .

applied in the H steady-state region near curve 4 in Figure 3.

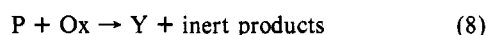
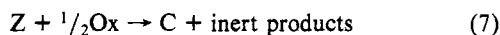
Figure 6 shows that there is a critical value above which the relaxation to the steady state occurs in a different way. This critical time of stopping of the inflow depends, for example, on the inflow concentration of bromate ion. Higher concentration results in a higher critical value. This phenomenon can be explained qualitatively as follows: When a perturbation is small, the system reaches a position which is close enough to the original steady state (node) and thus it will relax along a very simple trajectory to its original state. Different relaxation curves can result when the perturbation moves the system over the separatrix of the saddle point. Since there is only one attractor in the concentration space and this is the node, the system has to return to it even after such a perturbation. However, this can happen only on a longer course. The increase of the critical perturbation time indicates that the "distance" between the node and the separatrix becomes longer and longer as the input concentration of bromate ion is increased.

An improvement of this perturbation technique can give us the possibility in the future of determining the position of a further bifurcation point where the saddle and the other unstable steady state point (node or focus) disappear.<sup>12</sup> The exact determination of such a bifurcation point(s) in the phase diagram of the system is important from the point of view of checking the mechanistic explanations.

### Computations

The revised Oregonator type<sup>8,9</sup> and bromine-hydrolysis-controlled<sup>7</sup> skeleton model of the bromate-cerium-oxalic acid system

under CSTR conditions is given as follows:



The identifications are  $X = \text{HBrO}_2$ ,  $Y = \text{Br}^-$ ,  $P = \text{HOBr}$ ,  $W = \text{Br}_2$ ,  $Q = \text{BrO}_2^-$ ,  $\text{Ox} = (\text{COOH})_2$ ,  $C = \text{Ce(III)}$ ,  $Z = \text{Ce(IV)}$ , and  $A = \text{BrO}_3^-$ . The number of concentration variables was increased to nine since the inflow and outflow of the main components should also be involved in the modeling. According to Showalter et al.,<sup>19</sup> the autocatalytic generation of  $\text{HBrO}_2$  was broken down into two steps (reactions 3 and 4), one of which was made reversible.

The relevant differential equation for a component  $i$  is as follows

$$dc_i/dt = R(c_i) + k_0(c_{0,i} - c_i) \quad (10)$$

where  $c_i$  is the concentration of component  $i$ ,  $R(c_i)$  is its chemical mass action rate derived from the skeleton (except for reaction 7),  $k_0$  is the flow rate, and  $c_{0,i}$  is the inflowing concentration of the component. In the case of reaction 7 the experimentally determined rate equation<sup>20</sup> is

$$-\frac{d[\text{Ce(IV)}]}{dt} = -\frac{1}{2} \frac{d[(\text{COOH})_2]}{dt} = k_7[\text{Cr(IV)}][(\text{COOH})_2] \quad (11)$$

The resultant differential equation system was solved by Gear's method.<sup>21</sup> The applied rate constants are listed in Table I. Rate parameters from  $k_1$  to  $k_{-6}$  agree with the "0" set values<sup>22</sup> of the constants of the Noyes-Field-Thompson (NFT) model.<sup>23</sup> The experimentally found value of  $k_7$  ( $\sim 0.02 \text{ M}^{-1} \text{ s}^{-1}$  in  $1.0 \text{ M H}_2\text{SO}_4$ , ref 20) was modified according to Field and Boyd.<sup>24</sup> They demonstrated that the reduction of  $\text{Ce(IV)}$  by oxalic acid is 1000 times faster in the reaction system than in its equilibrium coordination state initially present. We applied the experimentally determined value of  $k_8$ .<sup>25,26</sup>  $k_9$  had to be increased to 0.1 for having oscillation in calculations applying the experimental conditions (input concentrations and flow rate).

The calculated and experimentally found bifurcation diagrams are shown in Figure 7. The most important difference is that no bistability was found by calculations in the concentration regions investigated experimentally. The shapes of the calculated oscillatory curves are completely different from that of the measured ones (not indicated here).

Figure 8 shows the measured and calculated dependences of time period on the inflowing bromate concentration under the same

TABLE I: Rate Constants for the Calculations<sup>a</sup>

$k_1 = 2.1 \text{ M}^{-1} \text{ s}^{-1}$	$k_6 = 8.0 \times 10^9 \text{ M}^{-1} \text{ s}^{-1}$
$k_2 = 2.0 \times 10^9 \text{ M}^{-1} \text{ s}^{-1}$	$k_{-6} = 110 \text{ s}^{-1}$
$k_3 = 1.0 \times 10^4 \text{ M}^{-1} \text{ s}^{-1}$	$k_7 = 20 \text{ M}^{-1} \text{ s}^{-1}$
$k_{-3} = 2.0 \times 10^7 \text{ M}^{-1} \text{ s}^{-1}$	$k_8 = 220 \text{ M}^{-1} \text{ s}^{-1}$
$k_4 = 6.5 \times 10^5 \text{ M}^{-1} \text{ s}^{-1}$	$k_9 = k_R = 0.1 \text{ s}^{-1}$
$k_5 = 4.0 \times 10^7 \text{ M}^{-1} \text{ s}^{-1}$	

<sup>a</sup>Hydrogen ion concentration was supposed to remain constant ( $1.0 \text{ M H}_2\text{SO}_4$ ) during the processes.

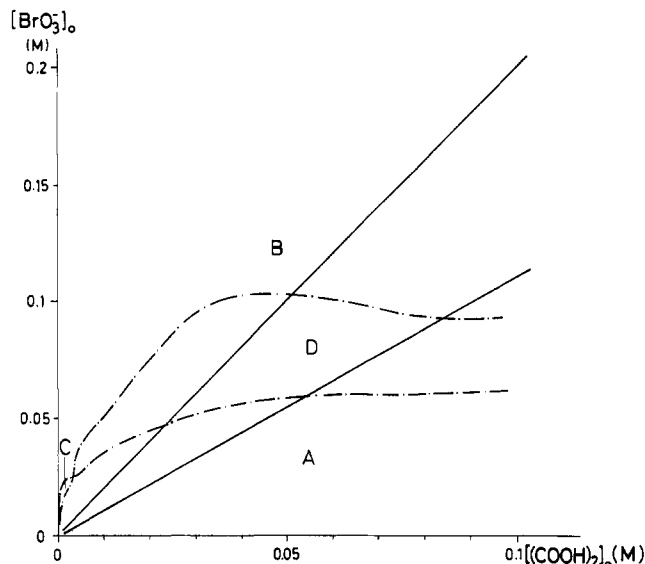


Figure 7. Calculated (—) and experimental (---) bifurcation diagrams. The parameters are the same as in Figure 3.

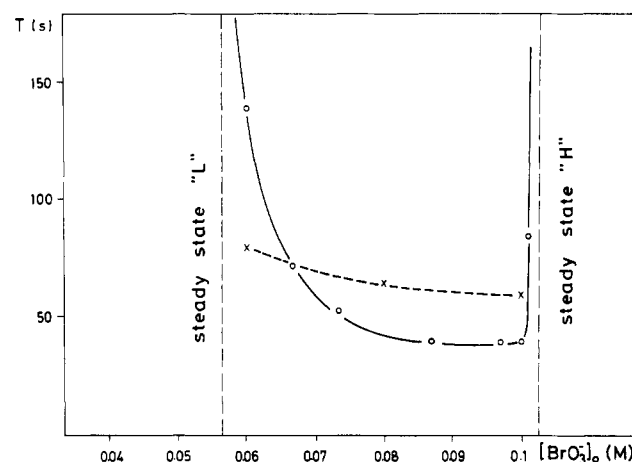


Figure 8. Calculated (x) and experimental (o) dependences of time period on the input concentration of bromate. Constraints:  $[(\text{COOH})_2]_0 = 5 \times 10^{-2} \text{ M}$  and others are the same as in Figure 3.

conditions. It turns out that in contrast to the experiments the time period tends to finite values in the vicinity of the bifurcation points in the calculations. The further results of calculations that the oscillations are ceased with finite amplitudes and some kind of hysteresis occurs during the transitions from limit cycle oscillations to steady states, and vice versa, indicate that bifurcations according to the model proceed by subcritical Hopf's ones.<sup>29</sup> The experimentally found excitability was not reached by calculations. (The resolutions in the calculations were at least the same as in the corresponding experiments.)

## Conclusions

The experimentally found SNIPER bifurcation in the bromate-cerium-oxalic acid system under CSTR conditions cannot be described by a revised Oregonator type<sup>8,9</sup> and bromine-hydrolysis-controlled<sup>7</sup> model. This type of skeleton resulted in subcritical Hopf's bifurcations. We hope that a more detailed

(19) Showalter, K.; Noyes, R. M.; Bar-Eli, K. *J. Chem. Phys.* **1978**, *69*, 2514-2524.

(20) Kansal, B. D.; Singh, N.; Singh, H. *J. Indian Chem. Soc.* **1978**, *55*, 304-307.

(21) Gear, C. W. *Numerical Initial Value Problems in Ordinary Differential Equations*; Prentice-Hall: Englewood Cliffs, NJ, 1971; pp 209-229.

(22) Bar-Eli, K.; Ronkin, J. *J. Phys. Chem.* **1984**, *88*, 2844-2847.

(23) Noyes, R. M.; Field, R. J.; Thompson, R. C. *J. Am. Chem. Soc.* **1971**, *93*, 7315-7316.

(24) Field, R. J.; Boyd, P. M. *J. Phys. Chem.* **1985**, *89*, 3707-3714.

(25) Knoller, Y.; Perlmutter-Hayman, B. *J. Am. Chem. Soc.* **1955**, *77*, 3212-3214.

(26) Smith, R. H. *Aust. J. Chem.* **1972**, *25*, 2503-2506.

mechanism of the system according to the recent results of Field and Boyd<sup>24</sup> will describe the experimentally found dynamic behavior of the system. Such calculations are in progress. Careful analysis of the peristaltic effect is also needed according to the results of Bar-Eli<sup>27</sup> and Taylor and Geiseler.<sup>28</sup> Since both the

(27) Bar-Eli, K. *J. Phys. Chem.* **1985**, *89*, 2852-2855.

(28) Taylor, T. W.; Geiseler, W. *Ber. Bunsenges. Phys. Chem.* **1985**, *89*, 441-446.

(29) One of our reviewers suggested that by applying the low set of rate constants our model would perhaps describe the SNIPER bifurcation behavior. One of our papers (ref 10) will show that a similar model of the batch reaction can result only in a Hopf bifurcation with the low set of rate constants, too. It is interesting to note that even the original irreversible Oregonator can show a saddle node transition in a very narrow region of the parameters. (DeKopper, P.; Boissonade, J. *J. Chem. Phys.* **1981**, *75*, 189-195.)

gas stream and the peristaltic pump can cause periodic or quasi-periodic effects, a similar investigation of dynamics of the bromate-cerium-oxalic acid-acetone system (in batch and in CSTR, too) is requested. Only such experiments can give us the possibility of deciding whether the observed peculiar dynamics originated from the chemistry of the system or from some special physical effects.

*Acknowledgment.* Dr. Z. Noszticzius and Dr. Gy. Bazsa are gratefully acknowledged for stimulating the experiments. We thank Professor M. T. Beck for his permanent interest and helpful recommendations.

Registry No. BrO<sub>3</sub><sup>-</sup>, 15541-45-4; Ce, 7440-45-1; H<sub>2</sub>C<sub>2</sub>O<sub>4</sub>, 144-62-7.

## High-Temperature Reactions of Triplet Methylene and Ketene with Radicals

P. Frank,\* K. A. Bhaskaran,<sup>†</sup> and Th. Just

*DFVLR Institut für Physikalische Chemie der Verbrennung, Stuttgart, West Germany*  
(Received: November 6, 1985)

The reactions of CH<sub>2</sub> and ketene with CH<sub>2</sub> and H have been investigated at elevated temperatures in the postshock region behind reflected shocks. Atomic (ARAS) and molecular resonance absorption spectrometry was used to record simultaneously H-atom and CO-molecule concentration profiles. The thermal decomposition of very low initial concentrations of ketene (2-50 ppm CH<sub>2</sub>CO/Ar) served as a source for methylene. The experiments were conducted in the temperature range of 1650-2800 K at total densities of  $5 \times 10^{-6}$  to  $1.3 \times 10^{-5}$  mol cm<sup>-3</sup>. For temperatures above 2000 K the following rate coefficients ( $k$  in cm<sup>3</sup> mol<sup>-1</sup> s<sup>-1</sup>) were deduced: CH<sub>2</sub> + CH<sub>2</sub> = C<sub>2</sub>H<sub>2</sub> + 2H,  $k = (10 \pm 2) \times 10^{13}$ ; CH<sub>2</sub> + H = CH + H<sub>2</sub>,  $k = (8 \pm 2) \times 10^{12}$ . For temperatures between 1650 and 1850 K a value of  $(1.8 \pm 0.6) \times 10^{13}$  is deduced for the reaction of ketene with H atoms.

### Introduction

The presence of methylene as an intermediate in many complex reaction systems proved to be of considerable importance to a detailed understanding of the underlying reaction mechanisms. In combustion processes CH<sub>2</sub> radicals are formed to some extent in the reaction of acetylene with oxygen atoms. Its subsequent reactions with other radicals and with oxygen are of fundamental interest for the mechanistic description of dominant reaction steps in combustion processes.<sup>1,2</sup> Most of the numerous experimental investigations—which are extensively reviewed in ref 3—were restricted to room temperature measurements, applying different techniques like flash photolysis coupled with time resolved vacuum-UV absorption spectrometry<sup>4</sup> or with product analysis by mass spectrometry<sup>5</sup> or gas chromatography.<sup>6,7</sup> Recent studies on reactions of triplet methylene with H and O in an isothermal discharge flow reactor at room temperature have been carried out by monitoring CH<sub>2</sub> radicals and O atoms with a far-IR laser magnetic resonance spectrometer.<sup>8,9</sup> Kinetic experiments in the system C<sub>2</sub>H<sub>2</sub>/O/H which were performed in a high-temperature discharge flow reactor coupled to a mass spectrometer<sup>1</sup> indicated that for temperatures up to 1300 K the temperature dependency of the rate coefficients for the reactions of methylene with acetylene or with hydrogen or oxygen atoms should be negligible or very small. From a shock tube study on acetylene oxidation in the temperature range 1500-2500 K, in which the measured H- and O-atom concentration profiles were simulated by a relatively small reaction mechanism, Loehr and Roth<sup>10</sup> derived high-temperature values for the fast subsequent reactions of methylene with H and O atoms. A first attempt to study in a more direct way high-temperature reactions of methylene has been performed in recent shock tube experiments on ethylene oxidation

by two of us.<sup>11</sup> In these experiments the source of methylene was the thermal decomposition of ketene. The interpretation of the measured H, O, and CO profiles concerning the methylene reactions was somewhat affected by the fact that at this stage of our research the initial concentrations of small amounts of ketene could not be measured directly, but were only deduced from the measured partial pressures during the filling of the storage tank.

### Experimental Section

Details of the shock tube as well as the optical setup have been described elsewhere<sup>12,13</sup> and only a brief summary will be presented here.

The brass shock tube consists of a test section of about 7 m in length and a driver section of 4 m. The internal diameter is 7.5 cm. The test section is evacuated by a turbomolecular pump to about 10<sup>-7</sup> mbar before each experiment. Mixtures are prepared and stored in a stirred 56-L stainless steel vessel which is bakeable

(1) Homann, K. H.; Wellmann, Ch. *Ber. Bunsenges. Phys. Chem.* **1983**, *87*, 609.

(2) Warnatz, J. *Ber. Bunsenges. Phys. Chem.* **1983**, *87*, 1008.

(3) Laufer, A. H. *Rev. Chem. Intermed.* **1981**, *4*, 225 and references therein.

(4) Braun, W.; Bass, A. M.; Pilling, M. *J. Chem. Phys.* **1970**, *52*, 5131.

(5) Vinckier, C.; DeBruyn, W. *Symp. (Int.) Combust., [Proc.]*, **17**, 1978 **1978**, 623.

(6) Laufer, A. H.; Bass, A. M. *J. Phys. Chem.* **1975**, *79*, 1635.

(7) Pilling, M. J.; Robertson, J. A. *Chem. Phys. Lett.* **1975**, *33*, 336.

(8) Boehland, T.; Temps, F.; Wagner, H. *Gg. Ber. Bunsenges. Phys. Chem.* **1984**, *88*, 455.

(9) Boehland, T.; Temps, F. *Ber. Bunsenges. Phys. Chem.* **1984**, *88*, 459.

(10) Loehr, R.; Roth, P. *Ber. Bunsenges. Phys. Chem.* **1981**, *85*, 153.

(11) Frank, P.; Just, Th. *Proc. 14th Symp. Shock Tubes Waves, Sydney* **1983**, 705.

(12) Just, Th. "ARAS in Shock Tubes" In *Shock Waves in Chemistry*; Lifshiz, A., Ed.; Marcel Dekker: New York, 1981.

(13) Frank, P.; Just, Th. *Ber. Bunsenges. Phys. Chem.* **1985**, *89*, 181.

\* Permanent address: Indian Institute of Technology, Madras, India.